MEMS Based Thin Film 2 GHz Resonator for CMOS Integration

Motoaki Hara, Jan Kuypers, Takashi Abe and Masayoshi Esashi

Department of Mechatronics and Precision Engineering, Tohoku University
01 Aoba, Aramaki-aza, Aoba-ku, Sendai 980-8579, Japan

Abstract — **This paper describes the development of the aluminum nitride (AlN) thin film bulk acoustic resonator (FBAR) using noble MEMS techniques for CMOS integration. This resonator has an air gap between a substrate for acoustic isolation. Germanium (Ge) was used as a sacrificial layer to make the air gap. This technique gives simple process and high CMOS compatibility. The resonator achieved a Q factor of 780 and an effective electro-mechanical coupling constant (k_{eff}^2) of 5.36 % at a resonant frequency of 2 GHz.**

I. INTRODUCTION

A drastic growth of the mobile markets demands smaller and cheaper RF-systems. Consequently, a CMOS compatible resonator is actively researched and developed all over the world[1]-[3]. The CMOS compatible resonator will allow realizing a one-chip front-end circuit and more integrated RF-systems. A thin film bulk acoustic resonator (FBAR) is a leading candidate of CMOS compatible resonators[4]-[6].

The FBAR is a bulk acoustic wave (BAW) device like a quartz resonator. It simply consists of plate electrodes and a piezoelectric film, and does not required any sub-micron patterns such as an interdigitated transducer (IDT) in a surface acoustic wave (SAW) device. Therefore, the FBAR obtains wider process margin and higher electrical performances, such as low insertion loss, high frequency operation and high power handling. The FBAR is fabricated on the substrate using conventional VLSI technologies, and substantially can be integrated to the CMOS circuit. But there are some problems which should be overcome to achieve full CMOS compatibility. How to achieve an acoustic isolation is one of them.

In order to obtain a high Q factor and reduce spurious responses, the FBAR has to be isolated acoustically from the substrate. The acoustic isolation structure falls into three types as shown in Fig. 1. In the configuration of Fig. 1 (a), there are the resonator on the diaphragm structure fabricated using a backside etching[4]-[6]. The (b) and (c) have an air gap[7] and acoustic multi-reflectors[8] between the resonator and the substrate, respectively. The air gap type resonator (AGR) and the solidity mounted type resonator (SMR) are fabricated by a surface process and suitable for CMOS integration. Especially, the AGR in which the acoustic isolation is achieved by the air allows theoretically higher Q factor than the SMR.

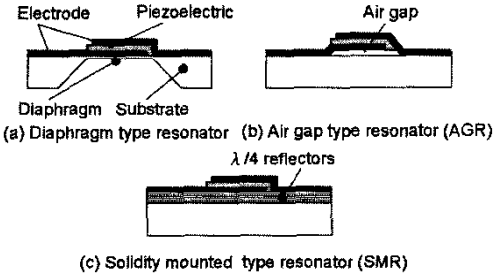

Fig. 1. acoustic isolation structures

A sacrificial layer etching is used for a free-standing structure formation. However, phosphosilicate-glass (PSG), porous-Si and a metal such as Al or Cu, which are commonly used as sacrificial layers, are not appropriate for a post CMOS processing, since these materials are etched by HF or HCl based solution which causes a defect of the CMOS circuit. Contrarily, germanium (Ge) is dissolved easily by hydrogen peroxide (H_2O_2) and provides good process compatibility as a sacrificial layer[9][10].

Both aluminum nitride (AlN) and zinc oxide (ZnO) are widely used for the FBAR as a piezoelectric layer, because those deposited films show high c-axis orientation, which is suitable for thickness vibration. AlN, especially, does not have a metal which performs the recombination center of the carriers such as zinc of ZnO. Hence, AlN is attractive for the CMOS integration. In addition, AlN film has several other advantages such as high breakdown voltages and low dielectric loss.

In this study, the air gap type FBAR has been fabricated using the Ge sacrificial layer etching and AlN as a piezoelectric layer.

II. FABRICATION

A. AlN Deposition

It is widely accepted that (111) plane of fcc metals such as Al, Au or Pt has geometric matching to hexagonal (002) plane of AlN. Since Pt does not generate an oxide and an alloy very well and obtains high (111) orientation when deposited easily[11][12], sputtered Pt was utilized as the base layer for AlN deposition. AlN was deposited using reactive sputtering under the condition shown in Table I.

0-7803-7695-1/03/$17.00 © 2003 IEEE

TABLE I
RF MAGNETRON REACTIVE SPUTTERING CONDITION FOR AlN DEPOSITION

Target	Aluminum (99.99 %), 2 inch
Substrate	Pt(111)/Ti/Si
Residual pres.	$<5\times10^{-8}$ Torr
RF power	200 W (10.2 W/cm^2)
Substrate temp.	400 °C
Sputtering pres.	1.0×10^{-1} Pa
Ar gas flow rate	28 sccm
N_2 gas flow rate	28 sccm
Deposition rate	24 nm/min.

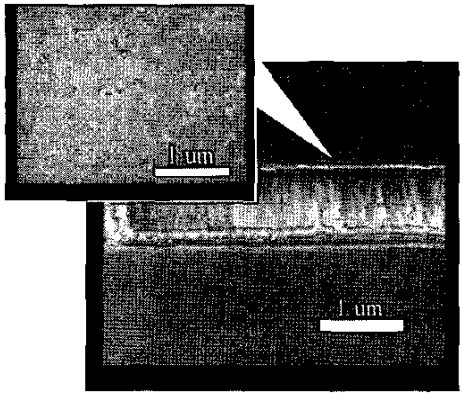

Fig. 2. SEM images of AlN film on Pt/Ti

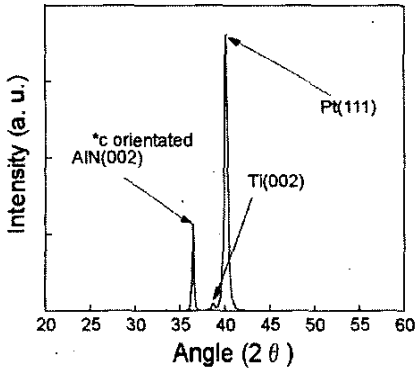

Fig. 3. XRD pattern of AlN film on Pt/Ti

Scanning electron microscopy (SEM) images of deposited AlN film are shown in Fig. 2. The film revealed the evidences indicative of zone-C-type morphology, that are columnar structure in cross section and grain facet on the surface[13]. An X-ray diffraction (XRD) pattern of the film clearly indicated AlN (002) peak as shown in Fig. 3.

B. Fabrication Of The Resonator

The schematic illustration and the process flow of the FBAR are shown in Fig. 4 and Fig. 5, respectively. After RCA cleaning, Ge is deposited as a sacrificial layer in thickness of 1.2 μm using an evaporator and patterned by H_2O_2 (Fig. 5 (a)(b)). A SiO_2 layer is deposited in thickness of 300 nm using plasma CVD (Fig. 5 (c)). The SiO_2 layer has a thermal stabilization effect of the resonance frequency because its positive temperature coefficient of frequency (TCF) compensates the negative TCF of the AlN[11]. Thin Ti layer (10 nm) and Pt layer (100nm) are deposited by sputtering as a bottom electrode, and seed layer for the AlN growth. The Pt layer is patterned by reactive ion etching (RIE), which can be used to etch Pt selectively with Xe, NH_3 and CO gas[14]. The Ti layer is etched by diluted HF (Fig. 5 (d)). After removing the resist, AlN is deposited by magnetron reactive sputtering and then etched photolithographically in diluted tetramethyl ammonium hydroxide (TMAH) at a temperature of 40 °C (Fig. 5 (e)). A top electrode of Pt/Ti is fabricated using the same technique as the bottom electrode (Fig. 5

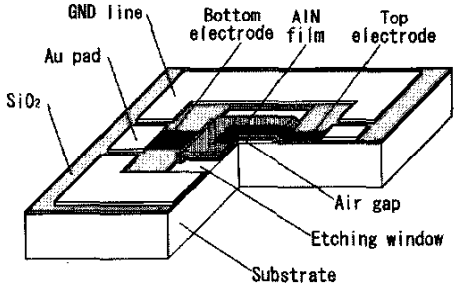

Fig. 4. schematic illustration of the FBAR

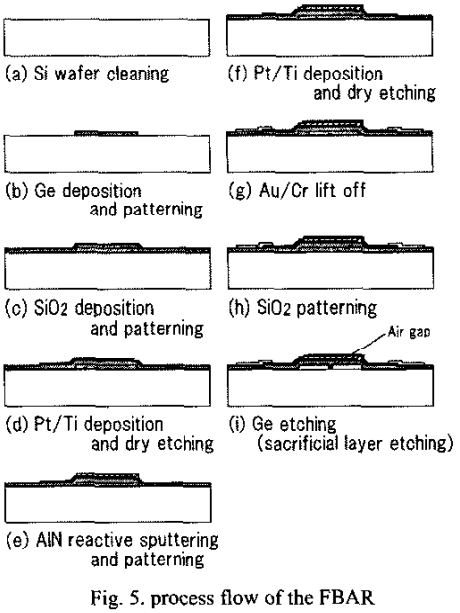

Fig. 5. process flow of the FBAR

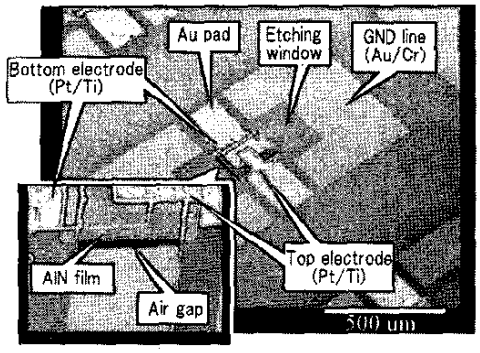

Fig. 6. SEM images of the fabricated FBAR

(f)). Au pads for the probing test are formed by lift off process (Fig. 5 (g)). SiO_2 is etched to expose the Ge and then Ge sacrificial layer beneath the resonator is removed by H_2O_2 (Fig. 5 (h)(i)). The fabricated resonator is shown in Fig. 6.

How to prevent a sticking to the substrate is a key issue for the free-standing thin film structure. The FBAR was rinsed and dried with Fluorinert (Sumitomo 3M) to obtain the free standing FBAR without sticking. Fluorinert indicates small surface tension and has been used for rinsing and drying of a free standing structure such as a micromachined cantilever[15].

III. Evaluation And Discussion

To confirm the availability of the air gap beneath the resonator, S-parameters of the FBAR with the air gap and without the air gap were measured and are shown in Fig. 7. Although S_{12} of the resonator without the air gap had many spurious peaks and did not have a resonance response, S_{12} of the resonator with air gap clearly had the resonance peak. Where, the AlN pattern area and thickness are 200 μm square and 1μm, respectively. The electrode area and thickness are 150μm square and 110 nm (Pt: 100 nm, Ti: 10 nm), respectively. The S-parameter of the FBARs was measured by ground-signal-ground prove system (Cascade Microtech: ACP110-CW).

Fig. 8 (a) and (b) show the S_{11} and the S_{12} of the FBARs having the electrodes of 150μm square, 100 μm square and 50 μm square, respectively. In Fig. 8, it is found that S_{12} of the FBAR decreases as the electrode area is reduced. This is because the impedance of the electrode capacitor is inversely proportional to the electrode area. The effect of an energy trapped mode was not observed. This is because the vibration energy was not trapped enough with only mass loading of the electrode. The energy trapped structure would have to be discussed.

The resonance of the FBAR can be characterized by the two figures of merit k_{eff}^2 and Q, where the k_{eff}^2 is the effective electro-mechanical constant constant and the Q is quality factor. Both the k_{eff}^2 and the Q of the FBAR

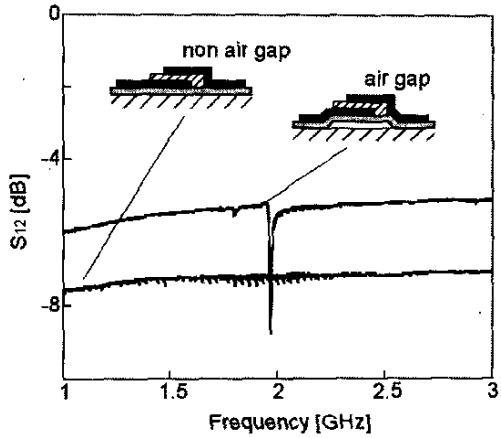

Fig. 7. the comparison between S_{12} of the FBAR with air gap and without air gap

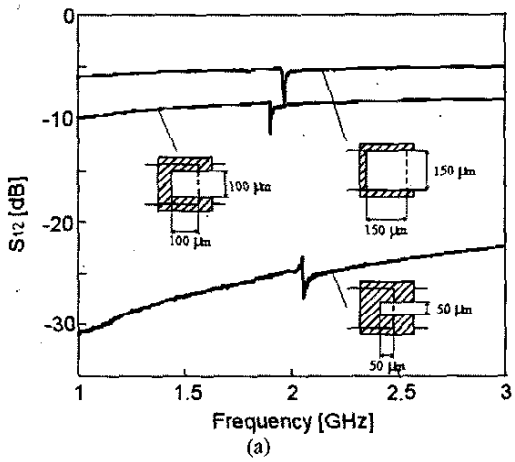

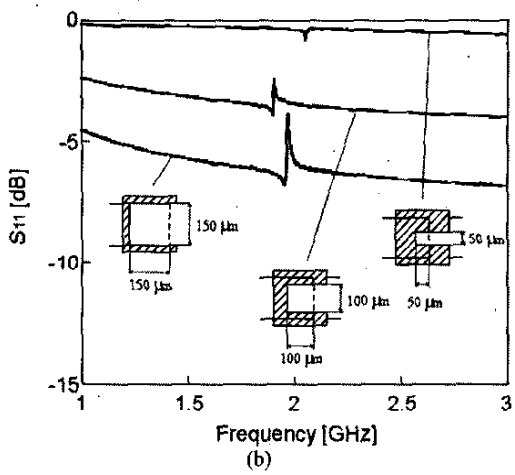

Fig. 8. the S_{11} and the S_{12} of the FBARs with different electrode areas

can be obtained from the S-parameter measurements as follows[16].

$$k_{eff}^2 = \frac{f_p^2 - f_s^2}{f_p^2} \quad (1)$$

$$Q = \frac{\left(\frac{f_s}{f_p}\right)}{1-\left(\frac{f_s}{f_p}\right)^2} \sqrt{\frac{\left(1-|S_{12\max}|\right)\left(1-|S_{11\min}|\right)}{|S_{12\max}|\quad |S_{11\min}|}} \quad (2)$$

Where f_p and f_s are parallel and series frequency of the FBAR, respectively. S_{12max} and S_{11min} are maximum value of measured S_{12} and minimum value of the measured S_{11}. In this study, from the experimental result and Eqs. (1)(2), the maximum k_{eff}^2 and Q were 5.36 % and 780, respectively.

IV. Conclusion

A CMOS integrated resonator is expected to realize a one-chip front-end circuit and to be applied to wireless communication systems or sensing systems.

For this purpose, a thin film bulk acoustic resonator (FBAR) isolated from the substrate acoustically with an air gap was fabricated. The piezoelectric layer of the FBAR is aluminum nitride (AlN) using reactive magnetron sputtering. The air gap is fabricated by surface micromachining using the germanium (Ge) as a sacrificial layer. The FBAR using AlN is compatible with CMOS circuit, because an Al of AlN does not cause a serious problem to CMOS process comparing zinc of ZnO and lead of PZT. Ge sacrificial layer etching technique is also compatible, because the Ge sacrificial layer is dissolved in H_2O_2, which does not attack CMOS circuit.

The fabricated resonator achieved a resonant frequency of 2 GHz, a Q factor of 780 and an effective electro-mechanical coupling constant (k_{eff}^2) of 5.36 %.

There are many problems to resolve in order to obtain the CMOS compatible resonator, which are deposition temperature, which is lower than 200 °C, thermal stability of the resonant frequency, yielding, reliability and packaging.

Acknowledgement

A part of this work was performed at VBL (Venture Business Lab.), Tohoku University, Japan. This work was supported in part by the Grant-in-Aid for Scientific Research from Ministry of Education, Scientific, Sports and Culture of Japan (13305010).

References

[1] R. C. Ruby, P. Bradly Y. Oshmyansky and A. Chien, "Thin film bulk acoustic resonator (FBAR) for wireless application," *Proc. IEEE Ultrason. Symp.*, pp 813 - 821, 2001

[2] P. Choi, S. Hyun, Y. Eo and K. Lee, "High Q VCO using an electro-acoustic device compatible with CMOS integrated circuit technology," *Proc. IEEE MTT-S*, pp. 913 - 916, 2000

[3] K. Wang, A-C. Wong and C-T-C. Nguyen, "VHF free-free beam high-Q micromechanical resonators," *IEEE J. Microelectromech. Syst.*, 9, pp. 347 – 360, 2000

[4] K. Nakamura, H. Sasaki and H. Shimizu, "A piezoelectric composite resonator consisting of a ZnO films on an anisotropically etched silicon substrate," *Jpn. J. Appl. Phys., 20 (Sippl. 20-3)*, pp 111 - 114, 1981

[5] K. M. Lakin and J. S. Wang, "Acoustic bulk wave composite resonators," *Appl. Phys. Lett.*, 38 (3), pp. 125 - 127, 1981

[6] T. W. Grudkowski, J. F. Black, T. M. Reeder, D. E. Culen and R. A. Wagner, "Fundamental-mode UHF/VHF miniature acoustic resonator and filters on silicon," *Appl. Phys. Lett.*, 37, pp. 993 – 995, 1980

[7] H. Satoh, Y. Ebata, H. Suzuki and C. Narahara, "An Air gap type piczoelectric composite resonator," *in 39th Annual Symp. Frequency Control Proc.*, pp. 361 -366, 1985

[8] K. M. Lakin, G. R. Kline and K. T. McCarron, "Development of miniature filters for wireless application," *IEEE Trans. Microwave Theory Tech.*, 43, pp. 2933 - 2939, 1995

[9] B. Li, B. Xiong, L. Jiang, Y. Zohar and M. Wong, "Germanium as a versatile material for low temperature micromachining," *IEEE J. Microelectromech. Syst.*, 8 (4), pp. 366 - 372, 1999

[10] J. M. Heck, C. G. Keller, A. E. Franke, L. Mulller, T. J. King and R. T. Howe, "High aspect ratio poly-silicon-germanium microstructures," *IEEE Transducers*, Sendai, Japan, pp. 328 - 331, 1999

[11] M. A. Dubois and P. Muralt, "Properties of aluminum nitride thin films for piezoelectric transducers and microwave filter applications," *Appl. Phys. Lett.*, 74(20), pp. 3032 - 3034, 1999

[12] M. A. Dubois and P. Muralt, "Stress and properties of aluminum nitride thin film deposited onto metal electrodes by pulsed direct current reactive sputtering," *J. Appl. Phys.*, 89(11), pp. 6389 – 6395, 2001

[13] J. A. Thornton, "Influence of apparatus geometry and deposition conditions on the structure and topography of thick sputtered coatings," *J. Vac. Sci. Technol.*, 11, pp. 666 - 670, 1974

[14] T. Abe, Y. G. Hong, K. Shinoda, N. Kobayashi, T. Yano and M. Esashi, "Micromachining of noble metal and magnetic metal thin films by RIE," *Proc. 19th Sensor Symp.*, Kyoto, Japan, pp. 337 - 340, 2002

[15] M. Ohtsu, K. Minami and M. Esashi, "Fabrication of packaged thin beam structures by an improved drying method," *IEEE Microelectromech. Syst.*, pp. 228 - 233, 1996

[16] Q. X. Su, P. Kirby, E. Komuro, M. Imura, Q. Zhang and R. Whatmore, "Thin-film bulk acoustic resonators and filters using ZnO and lead-zirconium-titanate thin films," *IEEE Trans. Microwave Theory Tech.*, 49(4), pp. 769 - 778, 2001